RADC-TDR-63-360

RADIATION CHARACTERISTICS OF A SIDE FIRE HELICAL ANTENNA

TECHNICAL DOCUMENTARY REPORT NO. RADC-TDR-63-360

October 1963

Techniques Laboratory
Rome Air Development Center
Research and Technology Division
Air Force Systems Command
Griffiss Air Force Base, New York

Project No.4506, Task No.450604

(Prepared under Contract No. AF30(602)-2646 by J. Perini, Syracuse University Research Institute, Electrical Engineering Department, Syracuse, N.Y.)

ABSTRACT

This antenna consists of a vertical conducting cylinder, 5λ long, and two conducting helices, of larger diameter, wrapped around it, with opposite pitches, starting at half of the cylinder length, the feed point, and progressing toward the ends.

It radiates mostly a horizontal polarized field. The horizontal pattern is approximately circular and the vertical forms a beam of 12° (gain 5). The bandwidth is over 10 percent. It has only one feed point on the 5λ aperture. It is very easy to build, self supporting, easily stacked to form an array and can also be used as self-diplexing.

. An exponentially decaying traveling current is assumed on the helices. The Fourier Transform method for reducing the problem to a two dimensional one was used successfully. Computed and experimental data are presented showing good agreement.

PUBLICATION REVIEW

This report has been reviewed and is approved. For further technical information on this project, contact Mr. J. Potenza, RALTM, Ext. 27147.

Approved: J. Potenza
J. POTENZA
Project Engineer
Directorate of Aerospace Surveillance & Control

Approved: Paul H Baldwin for Lt Col USAF
ARTHUR J. FROHLICH
Chief, Techniques Laboratory
Directorate of Aerospace Surveillance & Control

AIR FORCE, Cato Show Prtg. Co. 11/1/63 - 112 -

TABLE OF CONTENTS

Contents | Page

1. Introduction

The elements of this antenna are shown in Figure 1. It consists of a conducting cylinder C, approximately 5λ long and two conducting helices, H_1 and H_2, wrapped around it, at a certain distance from its surface. The two helices have the same pitch, in the order of $\frac{\lambda}{2}$, but of opposite signs and start at the feed point F progressing toward the ends of the cylinder.

A current is fed at the point F and travels along H_1 and H_2 radiating energy as it progresses. If the radius of the helix and of the cylinder are conveniently related, after five or six turns most of the energy is already radiated. The ends F' can therefore be left open-or short-circuited to the cylinder making very little difference on the performance of the antenna. Use of more than six turns is therefore a waste of aperture.

It has been determined experimentally that the rate of attenuation of the current depends mainly on the distance between the helix and the surface of the cylinder. It depends also on the diameter of the helix conductor.

If the cylinder C is in a vertical position, this antenna radiates mostly a horizontal polarized field. However, only when the length of a helix turn is an integral multiple of a wavelength the patterns have a useful shape. The horizontal pattern is roughly circular and the vertical pattern forms a nice beam of approximately 12° at half power (Figures 4-8). The frequencies at which this happens are referred to as moding frequencies of the antenna.

One of the nice properties of this antenna is its feeding system simplicity. It requires only one feed point for the 5λ aperture.

The impedance at the feed point F can easily be maintained under 1.1 VSWR over more than 10 percent bandwidth around the moding frequency. A typical plot is shown in Figure 2. By adjusting the slope of the helices at the feed point almost any point on the bandwidth can be brought to a perfect match. The patterns are also approximately constant over this bandwidth.

It is a very easy antenna to build. Requires only a few parts and can be made very rugged. The cylinder can be used as the supporting structure of the antenna making it self-supporting.

In some cases a tower can be used as the conducting cylinder. Screens have to be placed around it in order to improve the conductivity. The screens may be shaped to form a cylinder or may be flat on the tower. This will introduce modifications on the horizontal pattern mostly.

In places where the climate is such that ice is expected to be formed on the antenna, a 60 cps current may be circulated on the helix wire to prevent it.

This antenna offers also the possibility to be operated as a self diplexing antenna. There is no reason why the ends F' cannot be used as feed points. Therefore, a transmitter may be fed to F and another half to each end F'. If some precautions are taken, there will be very little cross coupling between the transmitters. The patterns are going to be somewhat different for the two transmitters because the current distribution is different when F or F' are used as feed points.

This antenna has been extensively used as a television transmitting antenna. It has also been used as the central station omni-directional transmitting antenna of communication systems.

2. Simplifying Hypothesis

In order to obtain the far field equations a model will be used and a certain number of simplifying hypothesis made.

The model is shown in Figure 3. The helices are substituted by a tape of width 2d and negligible thickness. The cylinder, as well as the helices, are of infinite length. This hypothesis will not describe the fact that standing waves exist on the helices due to reflections from the ends. This is not too important because the effect of the end reflections can be practically cancelled by shorting the end of one helix and leaving the other open or by making one of the helices $\frac{\lambda}{2}$ shorter than the other and leaving both ends open or short circuited to the mast.(1)

The simplifying hypotheses are:

(a) Both cylinder and tape helix are assumed to be perfect conductors.
(b) The current on the helix is assumed to be distributed uniformly throughout the tape width 2d.
(c) An exponentially decaying current is assumed to travel along both helices away from the feed point F.
(d) All fields are sinusoidally varying with time. In complex notation, the variation is of the form $e^{j\omega t}$.

Figure 3 shows some of the parameters used in the equations being derived here. These parameters are:

a - external radius of the conducting cylinder
b - radius of the helix cylinder
2d - tape width
p - helix pitch
n - number of wavelengths per turn

(1) The same techniques used here could be used to treat the problem of a finite length antenna. However, the equations would be much more difficult to handle algebraically.

3. Current Equations

The equation of the axis of the tape helix is

$$z = \frac{\phi}{2\pi} p; \quad \rho = b \tag{1}$$

If an exponentially decaying traveling current is assumed as both helices they can be written as:

$$J_{+}(z,\phi) = u(z) \frac{2C}{p} \sum_{m=-\infty}^{\infty} d_m e^{-\beta_m z} e^{-jm\phi} \tag{2}$$

in the z direction and

$$J_{-}(z,\phi) = u(-z) \frac{2C}{p} \sum_{m=-\infty}^{\infty} d_m e^{\beta_m z} e^{-jm\phi} \tag{3}$$

in the -z direction. In these equations

$$u(z) = 1 \quad z \geq 0. \tag{4}$$

$$= 0 \quad z < 0$$

$$\beta_m = \alpha + j(\beta - \alpha_m) \tag{5}$$

α and β being the attenuation and propagation constants of the current in the z direction. β can be written as

$$\beta = \frac{2\pi n}{p} \tag{6}$$

and

$$\alpha_m = \frac{2\pi m}{p} \tag{7}$$

$$d_m = \frac{\sin(\alpha_m d)}{\alpha_m} \tag{8}$$

C - current at the feed point

Equations (2) and (3) are obtained by considering the current pulses that appear in any plane passing through the z axis. Considering them of equal amplitude C it is possible to write its Fourier series representation and then multiply the result by $e^{-\alpha|z|}$. Depending upon which helix is considered this equation is multiplied either by $u(z)$ or $u(-z)$.

4. Construction of the Fields

The fields can be constructed by superposing TE and TM waves to z.[2] The appropriate potentials are

$$\text{TM:} \quad \underline{A} = \psi^{a}\, \underline{u}_z \quad * \tag{9}$$

$$\text{TM:} \quad \underline{F} = \psi^{f}\, \underline{u}_z \tag{10}$$

where ψ^{a} and ψ^{f} are suitable solutions of the Helmholtz equation, in cylindrical coordinates, for the regions $\rho \geq b$ and $a \leq \rho \leq b$. $\underline{u}_z$ is the unit vector in the z direction.

With $\underline{A}$ and $\underline{F}$ the fields are obtained from

$$\underline{E} = \frac{1}{\hat{y}}\left(k^2\underline{A} + \underline{\nabla}\,\underline{\nabla} \cdot \underline{A}\right) - \underline{\nabla} \times \underline{F} \tag{11}$$

$$\underline{H} = \frac{1}{\hat{z}}\left(k^2\underline{F} + \underline{\nabla}\,\underline{\nabla} \cdot \underline{F}\right) + \underline{\nabla} \times \underline{A} \tag{12}$$

where

$$\hat{y} = j\omega\epsilon \tag{13}$$

$$\hat{z} = j\omega\mu \tag{14}$$

The functions ψ^{a} and ψ^{f} may be written in a convenient form in the following way:[3]

$$** \begin{Bmatrix} \psi_e^{a} \\ \psi_e^{f} \end{Bmatrix} = \frac{1}{2\pi} \sum_{m=-\infty}^{\infty} e^{-jm\phi} \int_{-\infty}^{\infty} dw\, e^{-jwz} \begin{Bmatrix} A_m(w) \\ D_m(w) \end{Bmatrix} H_m^{(2)}(K\rho) \quad \text{for } \rho \geq b \qquad \begin{matrix} (15a) \\ (15b) \end{matrix}$$

and

(2) S.A. Schelkunoff, "Electromagnetic Waves," D. Van Nostrand Co., New York, 1936, p. 302.

*Underlined quantities are vectors.

**The subscripts e and i stand for the regions external or internal to the helix cylinder.

(3) J.A. Stratton, "Electromagnetic Theory," McGraw-Hill Book Co., New York, 1941, pp 355-364.

$$\begin{Bmatrix} \psi_i^a \\ \psi_i^f \end{Bmatrix} = \frac{1}{2\pi} \sum_{m=-\infty}^{\infty} e^{-jm\phi} \int_{-\infty}^{\infty} dwe^{-jwz} \begin{Bmatrix} B_m(w)J_m(K\rho) + C_m(w)N_m(K\rho) \\ E_m(w)J_m(K\rho) + F_m(w)N_n(K\rho) \end{Bmatrix} \text{for } a \leq \rho \leq b \qquad \begin{matrix} (16a) \\ (16b) \end{matrix}$$

where $K^2 = k^2 - w^2$
and A_m, B_m, C_m, D_m, E_m, F_m are functions of w to be determined from the boundary conditions. The other symbols are the usual notations for the Bessel Functions of first and second kind and the Henkel Function of second kind, all of order m.

5. The Fourier Transform Method

Tridimensional problems, having cylindrical symmetry, can be transformed into two-dimensional problems by taking the Fourier Transform in respect to the coordinate in the axis of symmetry.(4) If the function $\psi(x,y,z)$ is the solution of

$$\left(\frac{\partial^2}{\partial x^2} + \frac{\partial^2}{\partial y^2} + \frac{\partial^2}{\partial z^2} + k^2\right)\psi = 0$$

then the Fourier transform

$$\bar{\psi}(x,y,w) = \int_{-\infty}^{\infty} \psi(x,y,z)\, e^{-jwz}\, dz$$

will be a solution of the two-dimensional equation

$$\left(\frac{\partial^2}{\partial x^2} + \frac{\partial^2}{\partial y^2} + K^2\right)\bar{\psi} = 0$$

where

$$K^2 = k^2 - w^2$$

If the solution $\bar{\psi}$ is known or can be found then the solution of the tridimensional problem is obtained by inverting $\bar{\psi}$:

$$\psi(x,y,z) = \frac{1}{2\pi} \int_{-\infty}^{\infty} \bar{\psi}(x,y,w)\, e^{jwz} dw$$

When the potentials ψ^a and ψ^f were written in the previous section, the variation with z (the axis of symmetry) was chosen in such a way that the Fourier Transform can easily be written as

(4) R.F. Harrington, "Time-Harmonic Electromagnetic Fields," McGraw Hill Book Co., New York, 1961, pp. 242-245.

$$\left\{\begin{matrix} \bar{\psi}_e^a \\ \\ \bar{\psi}_e^f \end{matrix}\right\}^{*} = \sum_{m=-\infty}^{\infty} e^{-jm\phi} \left\{\begin{matrix} A_m(w) \\ \\ D_m(w) \end{matrix}\right\} H_m^{(2)}(K\rho) \quad \text{for } \rho \geq b \qquad \begin{matrix} (17a) \\ \\ (17b) \end{matrix}$$

and

$$\left\{\begin{matrix} \bar{\psi}_i^a \\ \\ \bar{\psi}_i^f \end{matrix}\right\} = \sum_{m=-\infty}^{\infty} e^{-jm\phi} \left\{\begin{matrix} B_m(w)\, J_m(K\rho) + C_m(w)\, N_m(K\rho) \\ \\ E_m(w)\, J_m(K\rho) + F_m(w)\, N_m(K\rho) \end{matrix}\right\} \qquad \begin{matrix} (18a) \\ \\ (18b) \end{matrix}$$

The Fourier Transform of the current, equations (2) and (3) are easily computed:

$$\bar{J}_{+} = \frac{2C}{p} \sum_{m=-\infty}^{\infty} d_m \frac{e^{-jm\phi}}{\beta_m + jv} \qquad (19a)$$

$$\bar{J}_{-} = \frac{2C}{p} \sum_{m=-\infty}^{\infty} d_m \frac{e^{-jm\phi}}{\beta_m - jv} \qquad (19b)$$

For future use on the boundary conditions it will be necessary to have the ϕ and z components of the current. If $\bar{J}_+$ and $\bar{J}_-$ are considered the ϕ component then

$$\bar{J}_{\phi} = \bar{J}_{+}\, \bar{J}_{-} = \frac{4C}{p} \sum_{m=-\infty}^{\infty} \frac{d_m\, \beta_m}{\beta_m^2 + v^2}\, e^{-jm\phi} = \sum_{m=-\infty}^{\infty} J_{\phi_m}\, e^{-jm\phi} \qquad (20)$$

$$\bar{J}_z = \frac{p}{2\pi b} (\bar{J}_{+} - \bar{J}_{-}) = -j \frac{2Cv}{\pi b} \sum_{m=-\infty}^{\infty} \frac{d_m\, e^{-jm\phi}}{\beta_m^2 + v^2} = \sum_{m=-\infty}^{\infty} J_{z_m}\, e^{-jm\phi} \qquad (21)$$

The definitions of J_{ϕ_m} and J_{z_m} are obvious from the above equations.

6. The Boundary Conditions

The boundary conditions are:

for $\rho = a$	$\bar{E}_{\phi}^{i} = 0$	(22)
	$\bar{E}_{z}^{i} = 0$	(23)
for $\rho = b$	$\bar{E}_{\phi}^{e} = \bar{E}_{\phi}^{i}$	(24)

* Variables with a bar on top are Fourier Transforms.

$$\bar{E}_z^e = \bar{E}_z^i \tag{25}$$

$$\bar{H}_\phi^e = \bar{H}_\phi^i = \bar{J}_z \tag{26}$$

$$\bar{H}_z^i = \bar{H}_z^e = \bar{J}_\phi \tag{27}$$

Substituting the Fourier Transforms of the potentials $\bar{\psi}^e$ and $\bar{\psi}^f$ in the Fourier Transforms of equations (11) and (12) the field components appearing in the boundary conditions are easily obtained. By inserting them in equations (22) through (27) a system of six equations, in the six unknowns A_m, B_m, C_m, D_m, E_m, F_m is obtained, the solution of which leads to:

$$\begin{Bmatrix} -A_m \\ -B_m \\ C_m \end{Bmatrix} = \frac{\omega h}{2H_{mb}^{(2)}} \left[\frac{-m\omega}{bK^2} \bar{J}_{\phi_m} + \bar{J}_{z_m} \right] \begin{Bmatrix} J_{mb}H_{ma} - J_{ma}H_{mb} \\ H_{ma}H_{mb}^{(2)} \\ J_{ma}H_{mb}^{(2)} \end{Bmatrix} \qquad \begin{matrix} (28) \\ (29) \\ (30) \end{matrix}$$

and

$$\begin{Bmatrix} D_m \\ E_m \\ -F_m \end{Bmatrix} = \frac{\omega b \hat{\imath}\, J_{\phi_m}}{2K\, H_{ma}^{(2)}} \begin{Bmatrix} J'_{mb}H'_{mb} - J'_{ma}H'_{mb} \\ H'_{ma}H_{mb}^{(2)'} \\ J'_{mb}H_{mb}^{(2)'} \end{Bmatrix} \qquad \begin{matrix} (31) \\ (32) \\ (33) \end{matrix}$$

Where the simplified notation for the Bessel and Henkel Functions

$$G_{ma} = G_m(aK)$$

has been used.

7. The Inversion Formula

It can be shown that if ρ is very large and θ is not equal to 0 or π, so that $\rho = r \sin \theta$ goes to ∞ as r goes, then the following equation is valid.(5)

$$\int_{-\infty}^{\infty} I(v)\, H_n^{(2)}\left(\rho\sqrt{k^2-v^2}\right) e^{jvz}\, dv \underset{\rho \to \infty}{\longrightarrow} 2\frac{e^{-jkr}}{r}\, j^{(n+1)}\, I(-k\cos\theta) \tag{34}$$

This is precisely the form of the inversion integral of equations (13), thus

(5) Silver and Saunders, "The External Field Produced by a Slot in an Infinite Circular Cylinder," J.A.P., Vol 21, No. 5, Feb. 1950, pp. 153-158.

$$\begin{Bmatrix} \psi_e^a \\ \\ \psi_e^f \end{Bmatrix} = \frac{e^{-jkr}}{\pi r} \sum_{m=-\infty}^{\infty} e^{-jm\phi} \, j^{(m+1)} \begin{Bmatrix} A_m(-k\cos\theta) \\ \\ D_m(-k\cos\theta) \end{Bmatrix} \quad \begin{matrix} (35a) \\ \\ (35b) \end{matrix}$$

where A_m and D_m are obtained from equations (28) and (31) substituting w by $-k\cos\theta$.

Expanding equations (11) and (12) in spherical coordinates, and retaining only the terms that vary as $\frac{1}{r}$, the following expressions result:

$$E_\theta = -\hat{z} A_\theta - jkF_\phi \qquad H_\theta = -\sqrt{\frac{\epsilon}{\mu}} E_\phi \qquad (36)$$

$$E_\phi = -\hat{z} A_\phi + jkF_\theta \qquad H_\phi = \sqrt{\frac{\epsilon}{\mu}} E_\theta \qquad (37)$$

where

$$A_\theta = -\psi_e^a \sin\theta \qquad A_\phi = 0 \qquad (38)$$

$$F_\theta = -\psi_e^f \sin\theta \qquad F_\phi = 0 \qquad (39)$$

Substituting (35a) and (35b) in (38), (39) and the result in (36), (37) the desired equations are obtained:

$$E_\theta = -\left|\hat{z}\right| \frac{e^{-jkr}}{\pi r} \sin\theta \sum_{m=-\infty}^{\infty} e^{-jm(\phi - \frac{\pi}{2})} A_m(-k\cos\theta) \qquad (40)$$

$$E_\phi = k \frac{e^{-jkr}}{\pi r} \sin\theta \sum_{m=-\infty}^{\infty} e^{-jm(\phi - \frac{\pi}{2})} D_m(-k\cos\theta) \qquad (41)$$

It is possible to show that the above series converges and that the important terms are the ones close to $|m-n| = 0$. A computer program was written to handle the problem and the results are presented in the next section.

8. Comparison With Experimental Results

Figures 4-7 show the comparison between measured (dashed) and computed vertical patterns (solid). The agreement for the E_θ component is good in the main beam region. The side lobe region does not agree because the reflections from the ends F' were not taken into consideration in the computations. The antenna was assumed to be of infinite length.

The value of α used on the computations was obtained experimentally. The measured E_θ patterns are not shown because it is difficult to measure them with reasonably good accuracy.

Figure 8 shows a comparison between measured (dashed) and computed horizontal patterns. In order to attenuate the effect of the reflections from the ends F' one of the helices was made $\frac{\lambda}{2}$ shorter. If this precaution is not taken, the horizontal pattern will present some scallops as shown in Figure 12. This is the case where a turn is 2λ long and there are four nulls and four maximums due to standing wave on the helices.

Figure 9 shows how the vertical pattern varies with the frequency. The phenomena of splitting the beam is well observed in the measurements as shown in Figure 10.

Figure 11 shows how the vertical pattern varies with α.

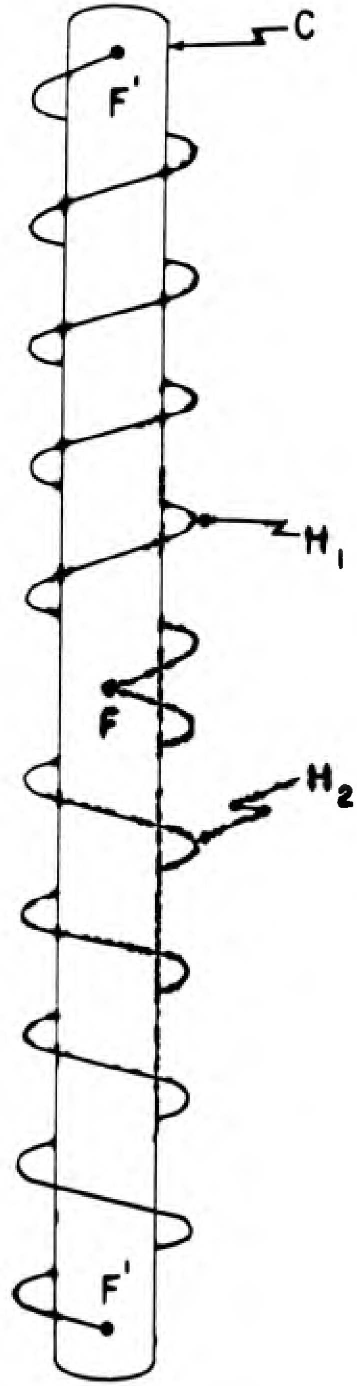

Figure. 1

ADMITTANCE COORDINATES

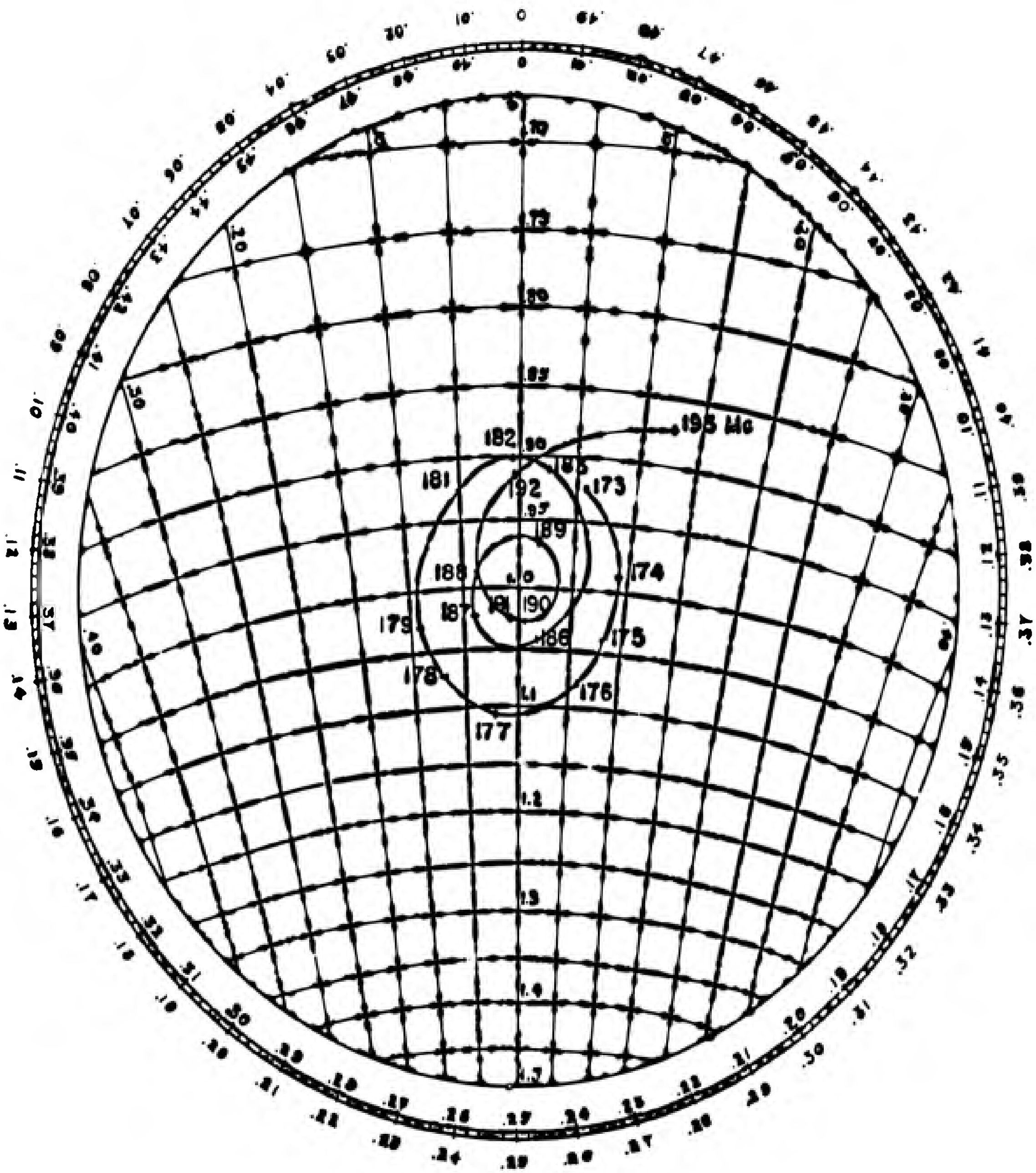

Figure 2. Input Admittance - Norm 50 Ω

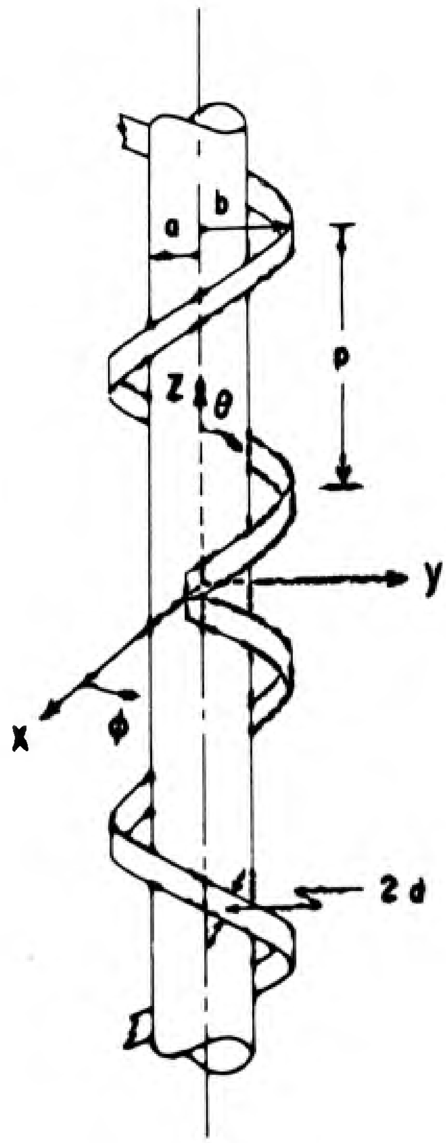

Figure. 3

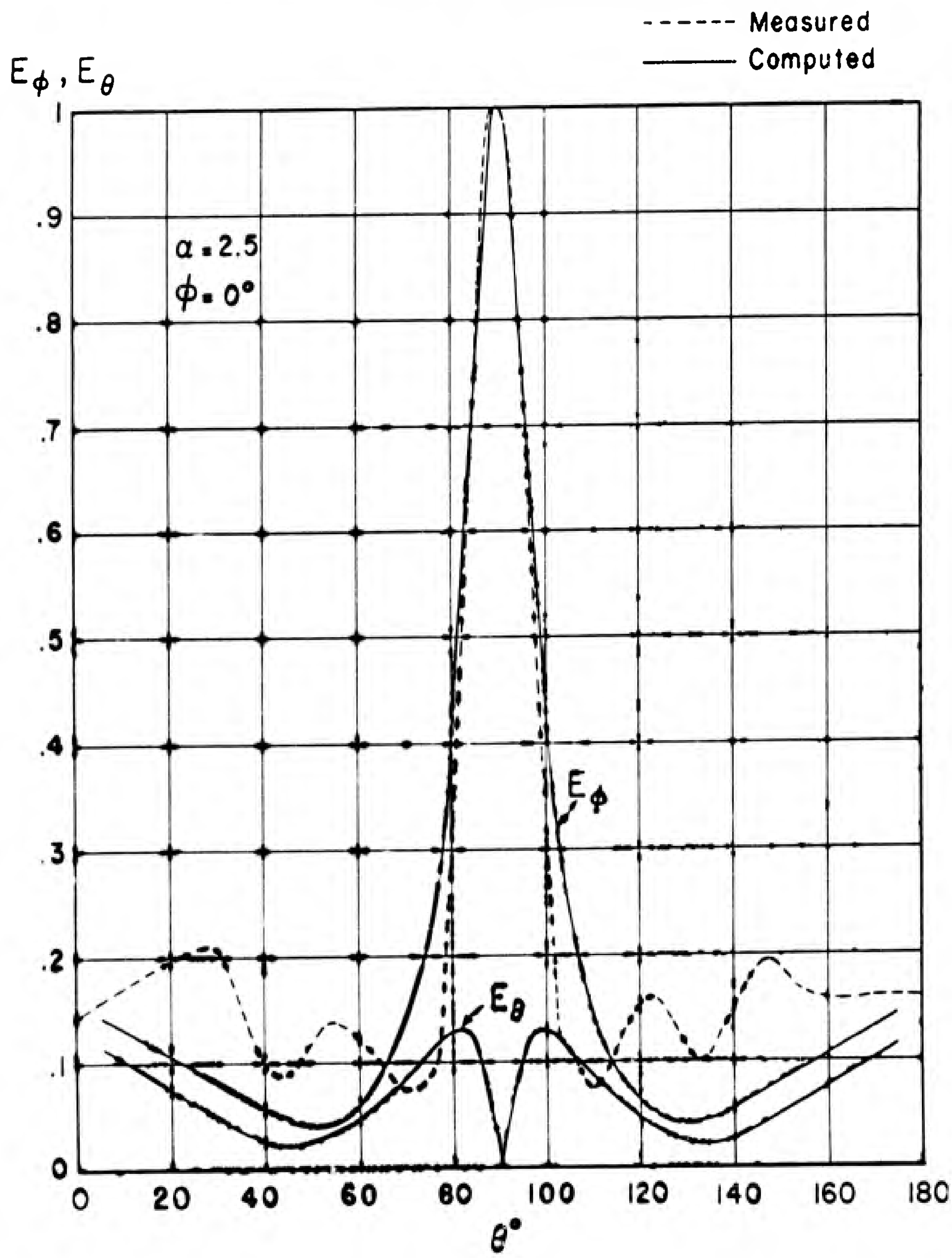

Fig. 4 Vertical Pattern

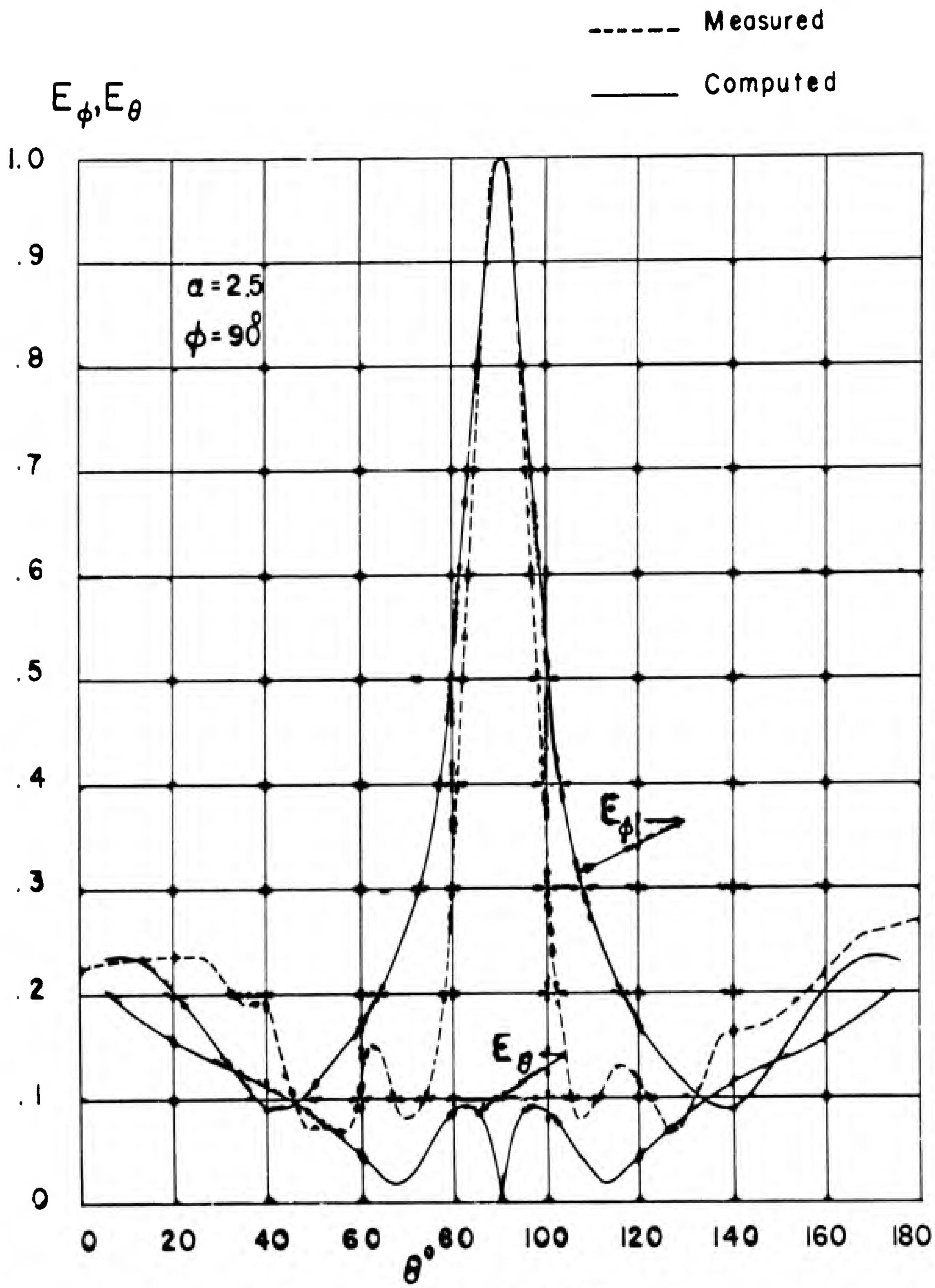

Fig.5 Vertical Pattern

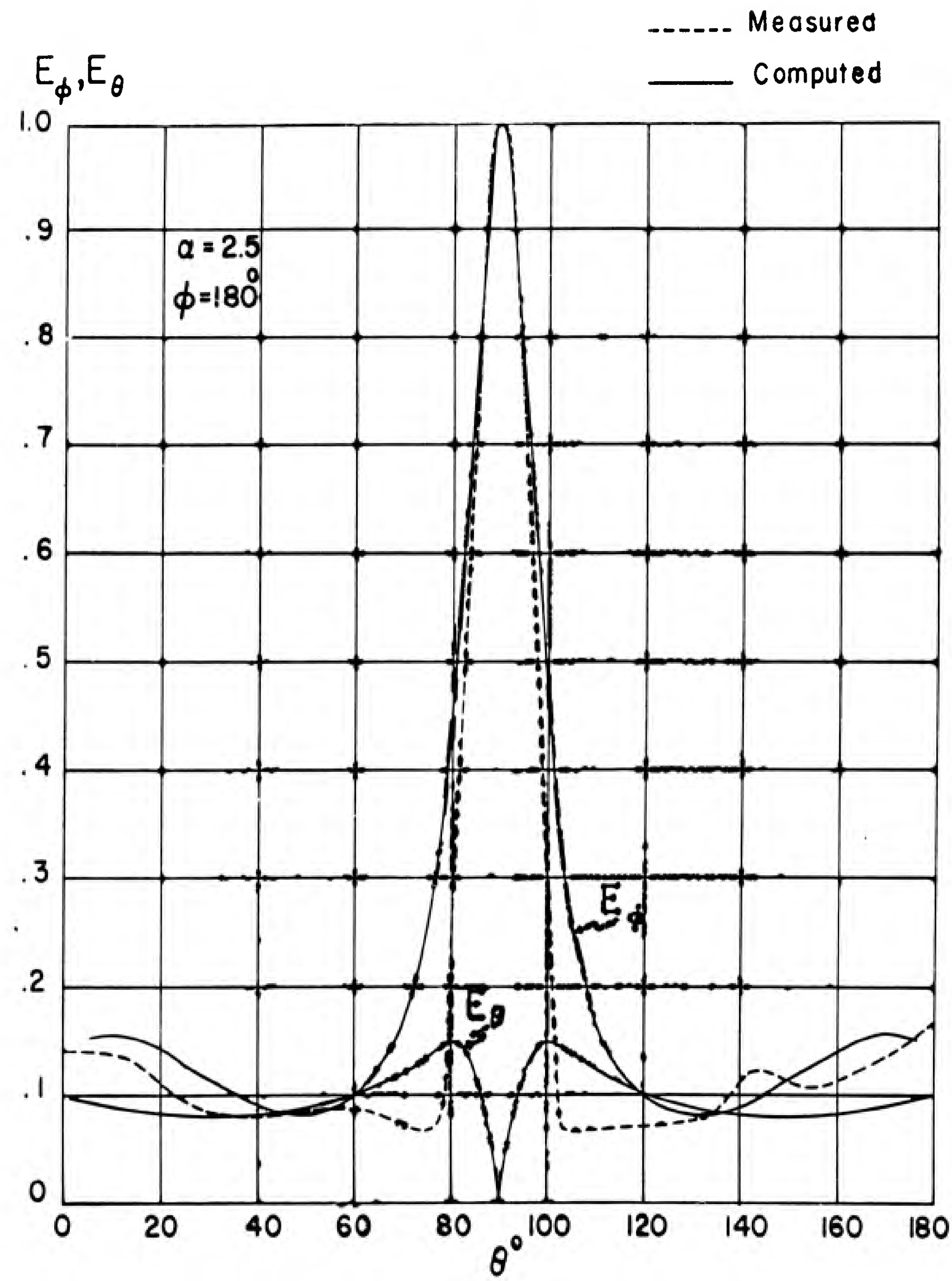

Fig. 6 Vertical Pattern

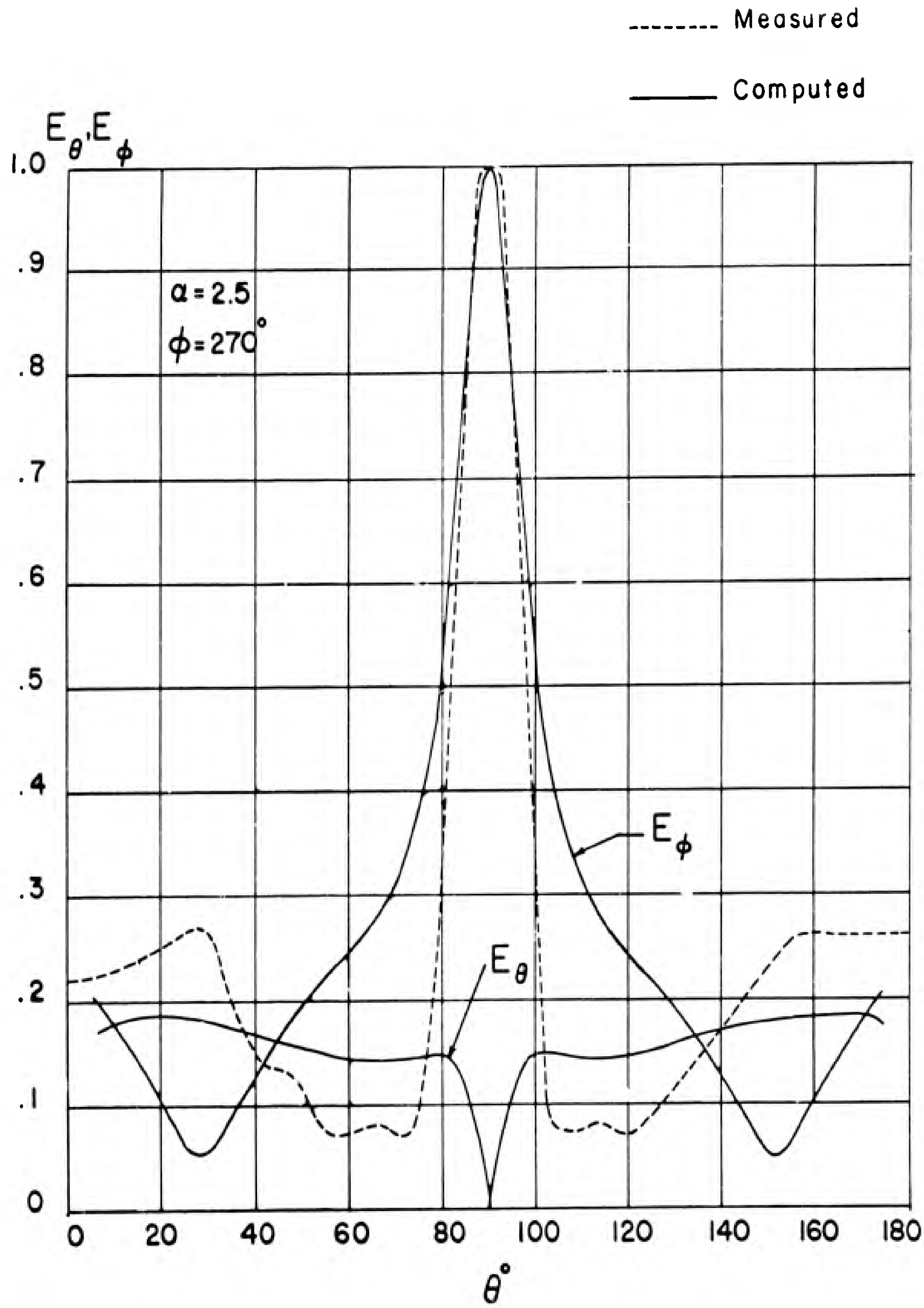

Fig.7 Vertical Pattern

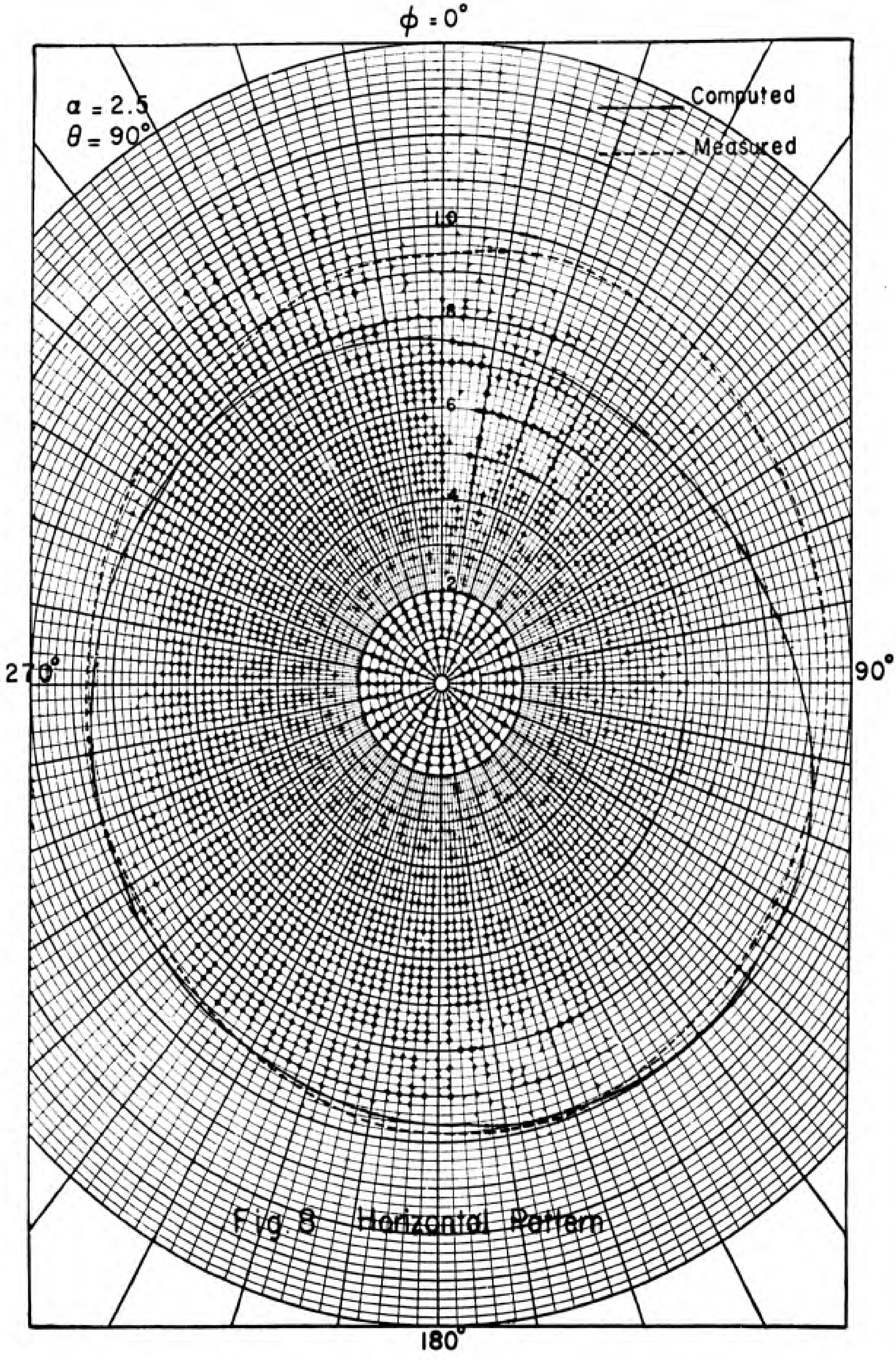

Fig. 8 Horizontal Pattern

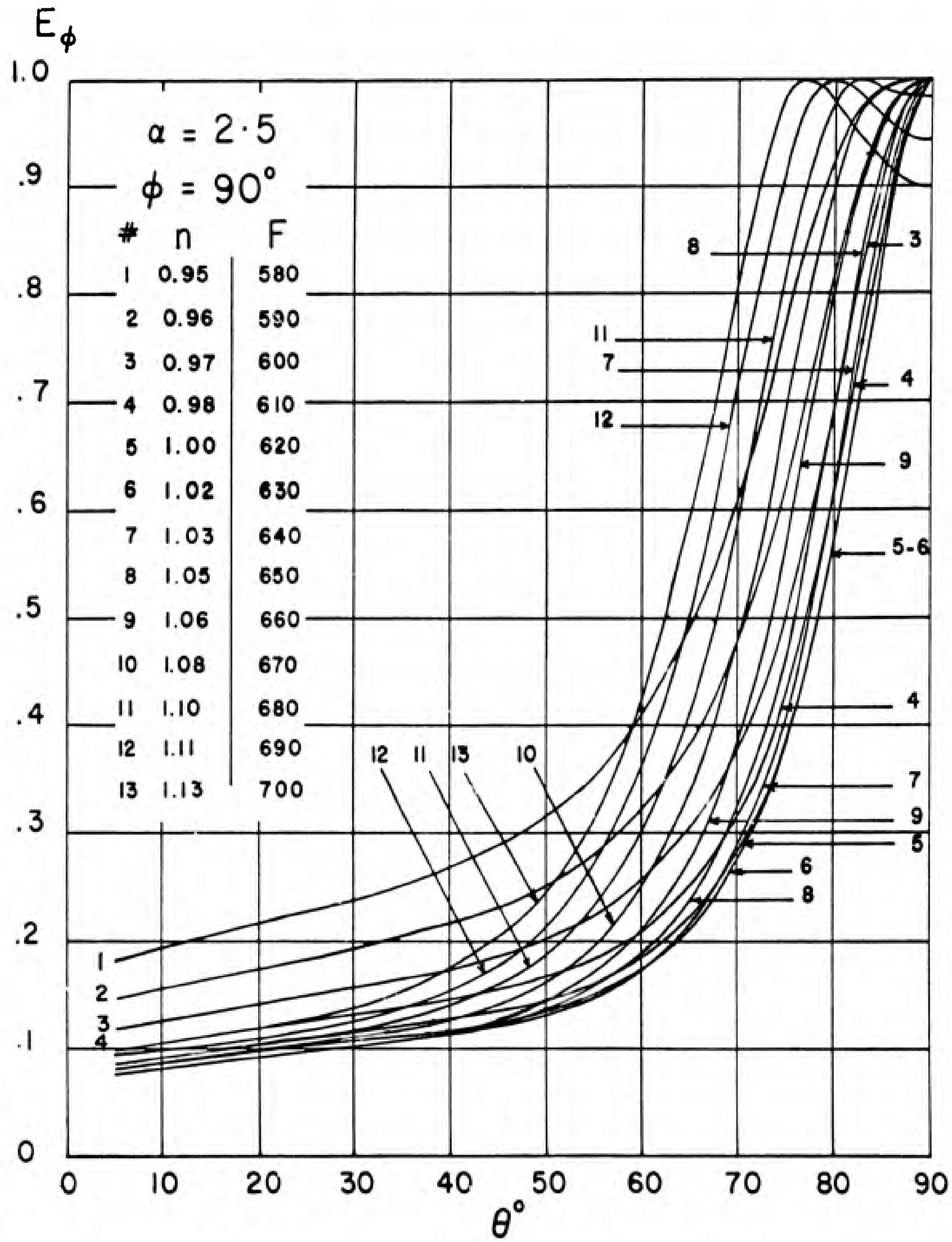

Fig. 9 Vertical Patterns

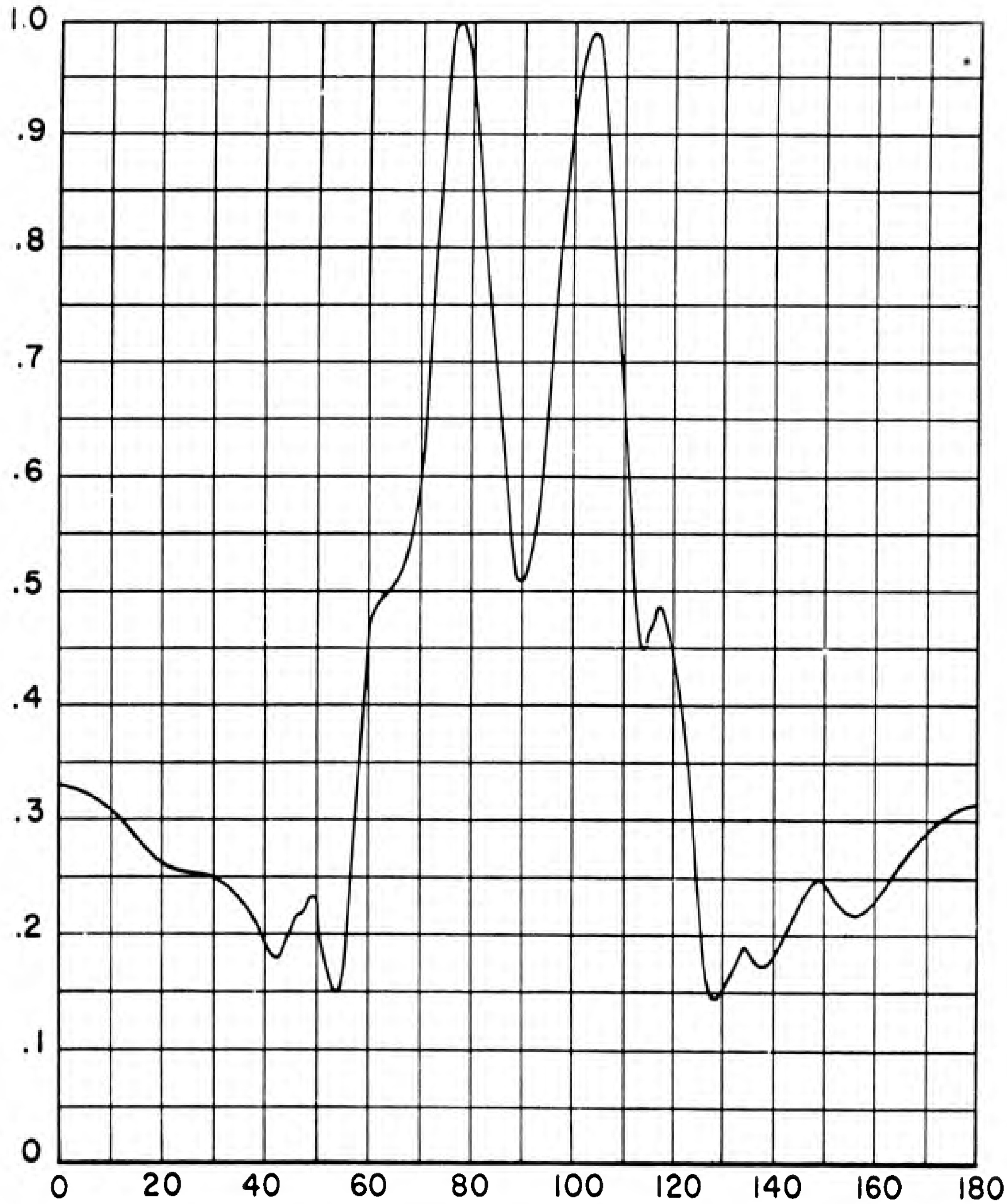

Fig. 10 Measured Vertical Pattern

One Wavelength per Turn Scale Model

F = 760 Mc.

n = 1.2

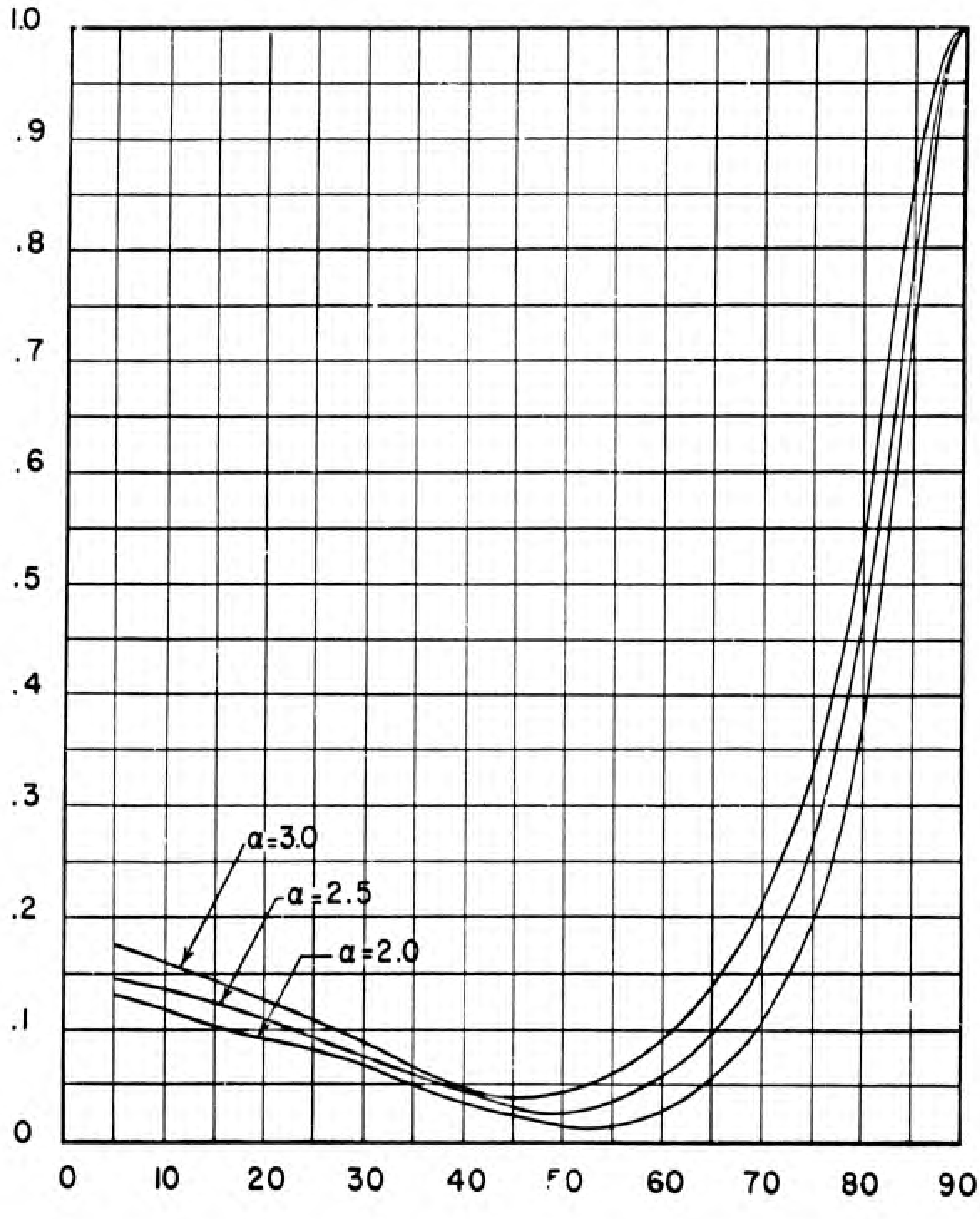

Fig. 11 Vertical Patterns
(Computed)
F = 750 Mc.
$\phi = 0°$

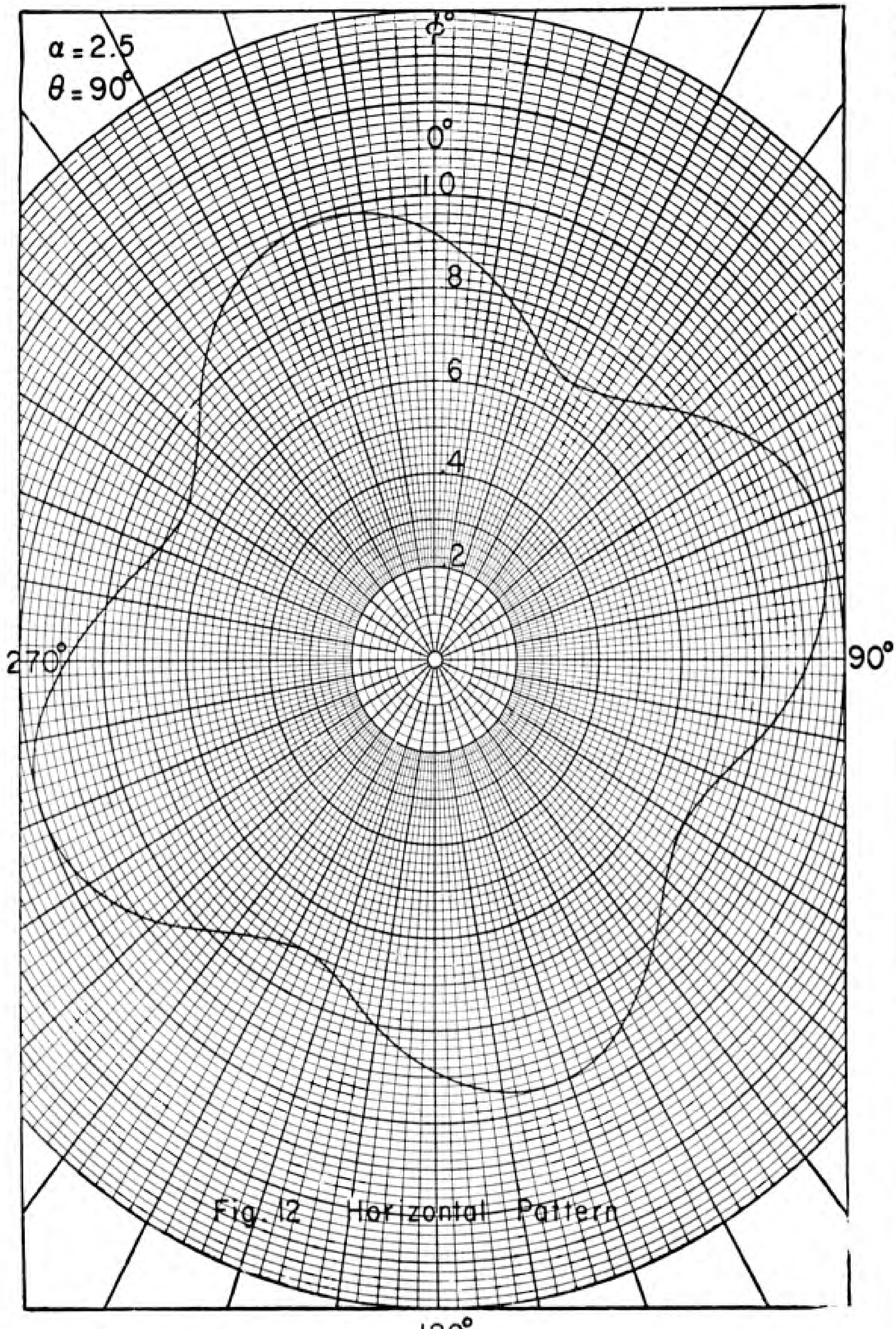

Fig. 12 Horizontal Pattern